bioRxiv preprint doi: https://doi.org/10.1101/456426; this version posted October 30, 2018. The copyright holder for this preprint (which was not certified by peer review) is the author/funder. All rights reserved. No reuse allowed without permission.

Age-dependent changes in transcription factor FOXO targeting in *Drosophila melanogaster*

Allison Birnbaum[1], Marc Tatar[2], Hua Bai[1]*

1 Department of Genetics, Development, and Cell Biology, Iowa State University, Ames, IA 50011, USA

2 Department of Ecology and Evolutionary Biology, Brown University, Providence, RI, 02912, USA.

Email:

Allison Birnbaum: abirnba1@iastate.edu

Marc Tatar: Marc_Tatar@brown.edu

Hua Bai: hbai@iastate.edu

***Corresponding Authors:**

Hua Bai

bioRxiv preprint doi: https://doi.org/10.1101/456426; this version posted October 30, 2018. The copyright holder for this preprint (which was not certified by peer review) is the author/funder. All rights reserved. No reuse allowed without permission.

Abstract

FOXO transcription factors have long been associated with longevity and tissue homeostasis. Although direct targets of FOXO have been reported in various long-lived mutants or stress conditions (nutrient deprivation), no studies have investigated how normal aging impacts the transcriptional activity of FOXO. Here, we conducted chromatin immunoprecipitation sequencing in both young and old wild-type fruit flies, *Drosophila melanogaster*, to evaluate the dynamics of FOXO gene targeting during aging. *Drosophila* FOXO binds to 2617 genes at young ages, whereas the number of FOXO-bound genes dramatically decreases to 224 at old ages. Consistently, many genes bound by FOXO in young flies are transcriptionally altered with age, including genes in Hippo and MAPK signaling pathways. Interestingly, we also find that many FOXO-bound genes in wild-type flies are unique from those in insulin mutants, suggesting FOXO is regulated by multiple upstream inputs. Together, these results provide new insights into dynamic FOXO targeting under normal aging and highlight the diverse regulatory mechanisms for FOXO transcriptional activity that are currently less understood.

Keywords: Forkhead transcription factor FOXO, ChIP-Seq, Transcriptional regulation, Longevity control

Introduction

The process of aging is accompanied by a decline in physiological function and cellular maintenance [1] [2]. It is known that aging dramatically alters gene expression and transcription factor activity [3]. The protein family of Forkhead Box subfamily O transcription factors, or FOXO, has been known to play a role in growth, development, stress resistance, and longevity [4]. FOXO functions downstream of insulin receptor and is negatively regulated by kinase Akt

bioRxiv preprint doi: https://doi.org/10.1101/456426; this version posted October 30, 2018. The copyright holder for this preprint (which was not certified by peer review) is the author/funder. All rights reserved. No reuse allowed without permission.

[5]. FOXO transcription factors control numerous pathways involving metabolism, cell cycle progression, stress, and apoptosis [6-9]. Additionally, FOXO proteins were first implemented in lifespan extension in *C. elegans* where insulin-like receptor mutant *daf-2* extends lifespan via FOXO homolog *daf-16* [10]. This lifespan extension through insulin/insulin-like growth factor signaling (IIS) has been observed across species, from worm to fly to mammal [10-12]. Studies have found in these organisms that dietary restriction or insulin deficiency is enough to promote FOXO nuclear localization and induce lifespan extension by targeting key longevity assurance pathways such as autophagy [13, 14]. However, a full comprehension of how FOXO elicits this response remains to be fully elucidated.

FOXO activity is not solely dependent on insulin activity. FOXO proteins undergo posttranslational modifications in response to other cellular stress signals. Oxidative stress can trigger Jun-N terminal Kinase (JNK) activation of FOXO in *Drosophila*, and mammalian Sterile 20-like kinase 1(MST1) activates *daf-16* in worms which allows for FOXO targeting of antioxidant genes [15-17]. In response to DNA damage, Cyclin-dependent kinase 2(CDK2) can phosphorylate and regulate FOXO1 to delay cell cycle progression and induce apoptosis [18]. FOXO proteins are also involved in tumor suppression activity and responds to oncogenic stress [15]. Interestingly, nuclear localization of FOXO has been observed not only under starvation or oxidative stress, but also under fed, non-stressed conditions [16, 19, 20]. Consistently, FOXO-DNA interactions were observed in both wild-type *C. elegans* and *Drosophila* [19, 21]

Despite many previous genomic analyses on DNA binding capacity of FOXO transcription factors and their target gene expression, the precise mechanisms underlying age-regulated FOXO transcriptional activity remain largely unclear. Here, we conducted a chromatin immunoprecipitation with next generation sequencing (ChIP-seq) analysis to investigate FOXO

bioRxiv preprint doi: https://doi.org/10.1101/456426; this version posted October 30, 2018. The copyright holder for this preprint (which was not certified by peer review) is the author/funder. All rights reserved. No reuse allowed without permission.

binding dynamics under normal aging in *Drosophila*. Intriguingly, FOXO-bound peaks with aging sharply decrease with age. The age-related decline of FOXO binding is correlated with the expression profile of many FOXO target genes during aging. Furthermore, we observed FOXO targets distinct sets of genes between wild-type flies and insulin mutants. Thus, our findings provide new evidence linking age-dependent FOXO transcriptional activity to its role in longevity control and tissue maintenance.

Results

FOXO exhibits constitutive nuclear localization in young and old adult fat body

Although mutations that block IIS and activate FOXO signaling often extend lifespan, how IIS and FOXO are altered during aging is not well characterized. To examine whether FOXO activity changes with aging, we first performed immunofluorescent staining using a polyclonal antibody against *Drosophila* FOXO (hereafter referred to as FOXO) to monitor the FOXO nuclear localization in wild-type flies at two different ages, two-week-old and five-week-old. Surprisingly, the abdominal fat body tissue of wild-type flies exhibited constitutive FOXO nuclear localization in both young and old flies (Figure 1A). It is also interesting that high levels of FOXO nuclear localization were observed in well-fed young flies, where insulin is presumably present and FOXO would be inactivated (Figure 1A). The constitutive nuclear localization of FOXO was also found in another wild-type line, *Oregon R* (*OreR*), but not in a *foxo* mutant line, *yw; +; foxo*^{21}. The total colocalization of FOXO with nuclear DAPI staining shows higher levels of nuclear FOXO in young flies compared to older and *foxo* mutant flies (figure 1B). Compared to adult fat body, indirect flight muscles from both one-week-old and

bioRxiv preprint doi: https://doi.org/10.1101/456426; this version posted October 30, 2018. The copyright holder for this preprint (which was not certified by peer review) is the author/funder. All rights reserved. No reuse allowed without permission.

five-week-old flies showed low overlap between FOXO staining and nuclear DAPI staining at both ages (Figure 1C & 1D).

We next conducted western analysis to distinguish changes in protein abundance with aging. The purpose of this is three-fold: first, to see if downstream targets of insulin signaling undergo post-translational changes with age. Second, to confirm FOXO protein expression with age, and thirdly, to verify our *foxo* mutant. We observed an increase in phosphorylated Akt protein with aging (Figure S1). We also saw FOXO protein expression in both the young and the old wild- type yw^{R} flies and confirmed a lack of full-length FOXO expression in $yw; +; foxo^{21}$ (Figure S1). Thus, we establish that FOXO protein is expressed under non-starvation conditions, and this expression persists with aging.

ChIP-seq analysis reveals age-dependent decline of FOXO-targeted DNA binding

To further investigate the transcription activity of nuclear localized FOXO under aging, ChIP-seq analysis on was performed using young (2-week) and old (5-week) female wild-type flies (Figure 2A). Using Illumina sequencing (HiSeq 3000, single-end, a read length of 50 base pair), we obtained a total of 261 million reads from 8 library samples. On average, 90.08% of unique reads were mapped to annotated Drosophila reference genome.

Intriguingly, our ChIP-Seq analysis revealed that the FOXO binding activity dramatically decreased with age, despite constitutive nuclear localization of FOXO at old age (Figure 2B&2D). For most of the peaks, a reduction in peak size or a disappearance of peaks altogether was observed in aged flies (Figure 2B). The strong reduction of FOXO-bound peaks was neither due to the reduced expression of FOXO protein (Figure S1A), nor the binding affinity between FOXO and genome. The aged fly shows more variable overall DNA concentrations of immunoprecipitated FOXO-bound chromatin compared to the young fly, with an average

bioRxiv preprint doi: https://doi.org/10.1101/456426; this version posted October 30, 2018. The copyright holder for this preprint (which was not certified by peer review) is the author/funder. All rights reserved. No reuse allowed without permission.

91.89% overall alignment to the Dm6 genome (Figure S2A and S2B). A comparative analysis of alignment data shows the 2-week-old FOXO ChIP samples to be most divergent from the non-immunoprecipitated input samples and 5-week-old ChIP samples, further supporting the decline of specific FOXO binding activity at old ages (Figure 2C).

Through FOXO ChIP-Seq, we identified 9273 FOXO-associated peaks from young flies (corresponding to 2617 unique protein coding genes), while only 1220 peaks corresponding to 224 genes were identified from old flies (Figure 2D). Pathway analysis revealed that FOXO target genes at young ages were enriched in pathways like Wnt, Hippo, MAPK pathways, and nervous system development and regulation (Figure 2D). FOXO was also targeting genes involved in synaptic tissue communication and motor neuron stabilization, such as Fascillin 2 (*Fas2*). Many of these peaks were absent in aged flies. Additionally, we found FOXO bound to genes that are important for autophagy regulation (Atg3, Atg17, Tor, wdb, Pten). Many Rho and small GTPase proteins appeared in our young FOXO dataset, suggesting a link between FOXO and the regulation of actin cytoskeleton. In the old flies, processes like cytokine mediation of inflammation and chromatin organization were enriched (Figure 2D). We found 170 shared target genes between two ages, with additional peaks enriched in old flies that did not overlap with the young dataset, suggesting that FOXO binding to specific pathways of growth and cellular maintenance are lost with age. FOXO binding at peak sites was verified by ChIP library preparation followed by gene specific qPCR. The promoter of the insulin receptor gene *InR* is known to be a target of FOXO [22]. Wild-type young fed flies showed no significant change in binding to the InR promoter compared to old flies (Figure 2E). Binding to the known FOXO-regulated gene *brummer* [23, 24] exhibited a decline in promoter binding with age (Figure 2F).

bioRxiv preprint doi: https://doi.org/10.1101/456426; this version posted October 30, 2018. The copyright holder for this preprint (which was not certified by peer review) is the author/funder. All rights reserved. No reuse allowed without permission.

This was compared to the ChIP-identified target Jim, which showed a significant 10-fold reduction with aging (Figure 2G), validating our ChIP results.

FOXO-bound genes show age-dependent transcriptional changes

We next examined whether age-dependent changes in FOXO binding is correlated to age-regulated transcription of FOXO target genes. To do so, we first compared our FOXO ChIP-seq results to previously published aging transcriptome data. Two *Drosophila* tissue datasets were used, one for transcriptional alterations in the aging fat body, and one for changes in head tissue with aging. We compared genes that were only present in the 2-week data set against the aging transcriptome profiles. From our 2447 FOXO-bound genes unique to young flies, we found 408 of them (15.3%) overlapping with the aging fat body transcriptome. 172 of these genes were downregulated, while a total of 236 genes were upregulated under aging (Figure 3A). A functional analysis of both overlapping gene sets revealed pathways involving neuroactive ligand-receptor signaling, peroxisome function, and Hippo signaling we both targeted by FOXO in young flies and also exhibited transcriptional changes with aging (Figure 3B, supplementary table 1). On the other hand, when comparing to aging head transcriptome data, we found that among 1450 genes that increase expression with aging, 219 of them were bound by FOXO only at young ages. Meanwhile, 626 of 1632 genes that were downregulated in the head showed overlap with FOXO ChIP-seq data (Figure 3C). These overlapping genes were enriched for functional processes involving Wnt, Hippo, insulin resistance, motor neuron axon guidance, MAPK/EGFR signaling (Figure 3D, supplementary table 1). 11 members of the defective proboscis extension response (Dpr) gene family as well as several Dpr-interacting protein (DIP) genes had altered regulation in the aging head and overlapped with FOXO binding (Supplementary table1). Many of these targeted genes that are involved in neuronal function and

bioRxiv preprint doi: https://doi.org/10.1101/456426; this version posted October 30, 2018. The copyright holder for this preprint (which was not certified by peer review) is the author/funder. All rights reserved. No reuse allowed without permission.

synaptic transmission are not present in the 5-week old flies, suggesting FOXO serves as a regulator of neuronal signaling in head tissue (supplementary table 1). Altogether, this data suggests that decreased FOXO-binding activity at old ages may contribute to age-dependent transcriptional changes of these FOXO target genes.

FOXO binding differs between wild-type and insulin mutants

FOXO binding activity has been primarily studied by evaluating its response to IIS signaling [19, 21, 25-27]. However, our observations on FOXO nuclear localization and DNA binding in well-fed wild-type flies suggest that there might be distinct FOXO transcriptional activity independent of IIS signaling. To test this, we compared FOXO ChIP-Seq datasets from the present study (young wild-type) and our previous analysis using *Chico* mutants [25]. Despite an overlap of 625 genes, there were 1992 genes unique to wild-type, and 1393 genes unique to *Chico* mutants (Figure 4A). Gene ontology analysis revealed that the overlapping set was enriched for processes involving synaptic transmission, cytoskeleton organization, and responses to endogenous stimuli. Both sets contained genes involved in the Hippo signaling pathway and the MAPK cascade, though different targets were apparent between the two datasets (Supplementary figure S4, S5, and S6). From the 1992 genes unique to the wild-type ChIP dataset, we found further enrichment of genes involving Hippo signaling and MAPK signaling (e.g., *Egfr, sev,* and *kay*), as well as enrichment of Wnt and Hedgehog signaling. Among the 1393 unique FOXO targets in *Chico* mutants, genes involved in metabolism were significantly enriched. We further compared the aging transcriptome datasets for head and fat body with FOXO ChIP-Seq results. About 844 age-regulated genes were bound by FOXO in wild-type flies, while 577 genes unique to *Chico* mutants (Figure 4B). We found that age-regulated FOXO target genes that are unique to *Chico* mutants were enriched for pathways in lipid metabolism

bioRxiv preprint doi: https://doi.org/10.1101/456426; this version posted October 30, 2018. The copyright holder for this preprint (which was not certified by peer review) is the author/funder. All rights reserved. No reuse allowed without permission.

and JNK signaling, while those unique to wild-type flies were enriched for Wnt signaling, Hippo signaling, and MAPK/EGFR signaling pathways (Figure 4C).

To test if distinct FOXO binding activity observed in wild-type flies is conserved across species, we compared our *Drosophila* FOXO ChIP-seq data with recent *C. elegans* Daf-16 ChIP-seq analyses. Intriguingly, wild-type worms also showed different Daf-16 binding activity from *daf-2* mutants. There were 2296 Daf-16 bound genes unique to wild-type worms, while 996 were unique to *daf-2* mutants (Figure 4D). Pathway analysis showed that both flies and worms exhibit FOXO and Daf-16 both target genes in pathways like cytoskeleton organization, axon guidance, and MAPK signaling (Figure 4E). The shared FOXO-targeting pathways found in wild-type flies and worms suggest that FOXO localization to target genes is not exclusively dependent upon insulin deficiency.

Enriched motifs from wild-type flies correspond with known FOXO co-factors

A hallmark of FOXO targeting is the 8-nucleotide long canonical binding motif 5'-TTGTTTAC-3' found across species [25, 28, 29]. This motif is typically found upstream of the gene coding site in the enhancer or promoter region [29, 30]. We conducted motif analysis using the Homer motif finding tool to search for FOXO consensus sequence in our ChIP-Seq data. For the 2-week wild-type flies, we used peaks with at least a 2-fold enrichment that were less than 2000bp in length, resulting in 5718 peaks. Using Homer to analyze genomic positions, we searched for motifs within 200bp surrounding the peak region. When using insect motif database, we found enrichment for only one known transcription factor motif, Trl ($p < 10^{-70}$), a GAGA-factor that also found in previous ChIP-seq data from *C. elegans* [21] (Figure 5). A *de novo* motif search revealed that FOXO-bound regions enriched with motifs for transcription factors hb, Adf1, and Aef1. Homer *de novo* motif search identified another motif for RAP1, a

bioRxiv preprint doi: https://doi.org/10.1101/456426; this version posted October 30, 2018. The copyright holder for this preprint (which was not certified by peer review) is the author/funder. All rights reserved. No reuse allowed without permission.

Saccharomyces cerevisiae gene that is part of the Myb/SAINT domain family, which is consistent with previous study by Alic et al 2011 [19]. However, Homer failed in detecting a canonical FOXO motif. When searching against known mammalian motifs, a motif for FOXO1 was detected with low significance ($p < 10^{-4}$) (Table 1). Therefore FOXO may recognize a unique motif in wild-type flies that is different from insulin mutants.

Discussion

As a key player in longevity control [10, 31, 32], FOXO transcription factors and their direct targets have been well characterized in many model systems [19, 21, 25, 27, 29, 30, 33, 34]. However, whether and how FOXO transcriptional activity changes with age is unknown. In the present study, we performed ChIP-Seq analysis to examine the FOXO binding activity during *Drosophila* aging. Intriguingly, whole genome FOXO-binding underwent an immense reduction at old ages, even though FOXO protein expression and nuclear localization did not show age-dependent changes. In addition, we found that FOXO presents in the nucleus of fat body tissue and binds to DNA under normal feeding conditions, suggesting FOXO is transcriptionally activated despite a lack of nutritional stress. Thus, we have discovered a novel age- and nutrition-independent FOXO transcriptional activation.

FOXO cofactors play an important role in FOXO differential DNA binding and transcriptional activity [16, 19, 21, 27, 35-37]. These co-factors include post-translational modifiers and nuclear interacting partners which aid FOXO in recruitment to target binding sites [38, 39]. We have seen in previous reports that FOXO targeted genes with age-differentiated expression are also targeted by other transcriptional regulators, suggesting that the interplay between FOXO and these transcription factors becomes altered during the aging process [27].

bioRxiv preprint doi: https://doi.org/10.1101/456426; this version posted October 30, 2018. The copyright holder for this preprint (which was not certified by peer review) is the author/funder. All rights reserved. No reuse allowed without permission.

Changes in transcription factor binding patterns at different stages of life are not exclusive to FOXO. In C. elegans, FoxA/PHA-4 exhibits differential binding patterns at different stages of development to regulate organogenesis. PHA-4 also exhibited binding at poised locations in the genome, similar to the observations made for FOXO in this study [40]. Our own data supports a loss of specific FOXO targeting with age, and this is possibly due to a decline in post-translational modifier activity and a reduction in FOXO-protein partner DNA binding. Certain mammalian FOXO cofactors, such as peroxisome proliferator-activated receptor gamma (PPARγ), and its coactivator (PGC-1α) interact with FOXO and compete for binding with FOXO and b-Catenin [41, 42]. FOXO acts as a repressor of PPARγ gene transcription, and this repression is lost later in life, suggesting a reduction of FOXO binding at this gene loci [42, 43]. This, along with other transcription factor co-regulators and post-translational modifiers influence FOXO's control of longevity [38, 44-46].

Target genes in young flies were functionally responsible for pathways involving growth, development, and cell maintenance as well as axon guidance and neuronal development. These pathways become transcriptionally altered with age. Young wild-type FOXO targets also showed unique genes and pathways when compared to FOXO targets identified in young *chico* mutants. FOXO binding has been previously linked to pathways involving tumorigenesis and regulation of cellular homeostasis [47]. One such pathway that is enriched among our wild-type FOXO targets is the Hippo signaling pathway. Genes involved in Hippo signaling were present in both wild-type and *chico* datasets, while further enrichment of the pathway was also found in the unique wild-type targets (Supplementary table 1, supplementary figure S4). Young fly FOXO targets that underwent a transcriptional change with age were also enriched for Hippo signaling. The Hippo pathway was initially characterized for its role in controlling organ size during

bioRxiv preprint doi: https://doi.org/10.1101/456426; this version posted October 30, 2018. The copyright holder for this preprint (which was not certified by peer review) is the author/funder. All rights reserved. No reuse allowed without permission.

development, but it also regulated pathways involving autophagy and oxidative stress response [48, 49]. These activities overlap with known FOXO functional behaviors [7, 20, 50]. In adult mice, suppression of Hippo signaling improved cell proliferation and heart tissue regeneration and is a regulator of tissue homeostasis [51]. These findings indicate Hippo signaling is targeted by FOXO and may regulate homeostatic activity, which becomes altered with age.

MAPK signaling is involved in tissue homeostasis with aging and was enriched among young FOXO-bound target genes [52, 53]. FOXO targets were found to correspond to both the EGFR and JNK cascades, and target genes involved in the EGFR pathway exhibited transcriptional alterations with age in the wild-type fly. In adult *Drosophila*, EGFR signaling is responsible for maintaining midgut epithelial homeostasis in the adult and has also been shown to regulate cytoskeletal modulation and autophagy [52, 54, 55]. EGFR regulation of autophagy also impacts glial maintenance and degeneration of the nervous system [53]. Our data supports FOXO targets the EGFR pathway and may serve as an upstream regulator of these processes.

Surprisingly, we found many FOXO-bound peaks appeared at histone coding regions, and this number increased with age. This suggests FOXO has some involvement in the maintenance of chromatin structure. This is supported by previous research highlighting that FOXO recruits SWI/SNF chromatin remodelers to specific target sites [21]. Changes in chromatin structure and overall loss of heterochromatin has long been an indicative measurement of aging [56-58]. Therefore, it is possible that FOXO is required for maintaining chromatin structure and may serve as a repressor for specific gene targets.

In summary, using a genome-wide approach we were able to observe the dynamic nature of FOXO binding, and found an overall reduction of gene targeting with age in the wild-type fly. Our findings support FOXO as important regulator of processes that undergo changes with age.

bioRxiv preprint doi: https://doi.org/10.1101/456426; this version posted October 30, 2018. The copyright holder for this preprint (which was not certified by peer review) is the author/funder. All rights reserved. No reuse allowed without permission.

This reinforces FOXO's role in the regulation of homeostasis and cellular maintenance pathways. Further investigation of the function of this decline in FOXO binding with age will be important in understanding how FOXO regulates organismal homeostasis and longevity.

Methods

Fly lines

ywR;+;+ (Rochele) flies were used as wild-type for ChIP-seq. *ywR;+:foxo*^{21} line serves as FOXO mutant flies. Females were collected and sorted 1-2 days after eclosion and placed in vials containing standard CSY food. Fly strains were maintained at 25 ℃ with 12 hour light/dark cycle, and 60% humidity. Vials contained 25-30 flies to prevent overcrowding and were transferred to fresh food every three days. Flies were aged to 2-weeks old (12-14 days) for both ywR and foxo^{21} mutant lines, and 5-weeks old (34-36 days) for ywR aged specimens.

Immunofluorescent staining

Flies were subjected to flynap (Carolina, Burlington, NC) and dissected in 1X phosphate buffer saline (PBS). Tissue was then fixed in 4% paraformaldehyde for 20 minutes at room temperature. Tissue was washed in 1X PBST (0.1% Triton X) and blocked with 5% NGS for 1 hour at room temperature. Tissue was stained with α-FOXO antibody (Tatar Lab) in 1X PBST at a dilution of 1:1000 for 16 hours at 4 ℃ on a rotator. Tissues were placed in secondary anti-body goat-anti-rabbit conjugate Alexa Fluor 488 (Jackson ImmunoResearch Laboratories Inc, West Grove PA) at a Dilution of 1:250 and kept in the dark at room temperature for 2 hours. The nucleus was stained using SlowFade with DAPI () and tissues were stored at 4 ℃ overnight prior to plating. Images were captured using an epifluorescence-equipped BX51WI microscope

bioRxiv preprint doi: https://doi.org/10.1101/456426; this version posted October 30, 2018. The copyright holder for this preprint (which was not certified by peer review) is the author/funder. All rights reserved. No reuse allowed without permission.

298 (Olympus, Waltham, MA, USA). and CellSens software (Olympus, Waltham, MA, USA) for
299 deconvolution. Images were compiled using Fiji [59].

300 *ChIP*

301 ChIP-PCR protocol was performed and modified from [25]. Two biological replicates were
302 collected for each age and genotype. For Crosslinking, ~200 female flies were anesthetized with
303 Flynap (Carolina, Burlington, NC, USA) and ground into a powder in liquid nitrogen.
304 Crosslinking was allowed for 20 minutes in 1X PBS with 1% paraformaldehyde before quenched
305 with glycine. Chromatin was washed several times with 1X PBS supplemented with protease
306 inhibitor (PIC). Pellets were washed once with cold cell lysis buffer (5mM HEPES pH7.6,
307 100mM NaCl, 1M EDTA,0.5% NP-40, ddH2O, 0.1% PIC). Buffer was removed and samples
308 were snap frozen in liquid nitrogen and stored at -80 ℃ to synchronize experiments. Samples
309 were thawed and treated with nuclear lysis buffer (50mM HEPES pH7.6, 10mM EDTA, 0.1%
310 Na-deoxycholate, 0.5% N-lauroylsarcosine, ddH2O, 0.1% PIC) and incubated at 4 ℃ for 10
311 minutes. Chromatin was sheared for 500bp using Branson digital sonifier 250, using 30%, with
312 30 seconds on 30 seconds 0ff for 5 cycles. Supernatant was snap frozen and stored at -80 ℃.
313 Immunoprecipitation was carried out using Protein-G SureBeads (BioRad Hurcules, CA, USA).
314 Beads were washed once with 1X PBS prior to blocking with 1X PBS and 0.5% BSA for 20
315 minutes at 4 ℃. Samples were precipitated with affinity purified anti-dFOXO antibody (Tatar
316 Lab). Samples were reverse crosslinked at 65 ℃ for 12 hours.
317 DNA size selection and library prep were done using NEBNext Ultra II DNA library prep kit for
318 Illumina an indexed using NEBNext multiplex oligos for Illumina (Primer set 1) (New England
319 BioLabs, Ipswich, MA, USA). DNA from either ChIP or input samples was mixed with AMPure
320 XP beads (Beckman Coulter, Inc. Brea, CA, USA) to select for a final library size of 320bp.

bioRxiv preprint doi: https://doi.org/10.1101/456426; this version posted October 30, 2018. The copyright holder for this preprint (which was not certified by peer review) is the author/funder. All rights reserved. No reuse allowed without permission.

Samples were diluted to a final concentration of 2nM for Illumina sequencing on Illumina 3000 (Illumina, San Diego, CA, USA).

Processing of ChIP-seq data

Raw FASTQ reads were merged using mergePeaks (Homer suite) then uploaded into Galaxy (usegalaxy.org) and checked for quality using FastQC (Andrews; figure S*). Files were then run through FASTQ Groomer (https://usegalaxy.org/u/dan/p/fastq) for readability control before mapping reads using Bowtie2 for single-end reads (Langmead and Salzberg 2012). D. melanogaster Aug.2014 (BDGP Release 6 + ISO1 MT/dm6) was used as the reference sequence. BAM output files were converted to SAM using BAM-to-SAM (http://www.htslib.org/doc/samtools.html) and sorted (Li 2009, SAMTools) to generate peak images in Figure 2C. Peak calling was performed using MACS2. MACS2 FDR (q-value) was set for a peak detection cutoff of 0.05 and did not build the shifting model. The MFOLD for the model was set from 10-50 to detect fold-enrichment as specified by Feng et al 2012 [60]. Peak-calling was set to identify peaks 300bp in length, and no peaks could exceed 10Kb in size. After MACS2 peak identification, peak regions were expanded 2kb (1kb upstream and downstream) and assigned to nearby and overlapping genes using BEDTools/intersect (https://bedtools.readthedocs.io/en/latest/content/bedtools-suite.html) with dm6.16 genome annotation file (UCSC, Santa Cruz, CA, USA). All non-protein coding identified targets were removed from the data set manually based on annotation symbol (CG vs CR).

Venn Diagrams

Venn diagram were created using the Bioinformatics and Evolutionary Genomics Venn calculator at Ugent (http://bioinformatics.psb.ugent.be/webtools/Venn/). For cross species

bioRxiv preprint doi: https://doi.org/10.1101/456426; this version posted October 30, 2018. The copyright holder for this preprint (which was not certified by peer review) is the author/funder. All rights reserved. No reuse allowed without permission.

comparisons, gene ID's were converted to fly ID's using DIOPT (http://www.flyrnai.org/diopt). Genes that were the best possible match for each ortholog were selected for gene list comparison.

qPCR

Quantitative PCR was run on ChIP purified samples (QuantStudio, ThermoFisher Scientific, Waltham, MA USA). Cybergreen (Life Technologies, CA, USA) was used for chemical detection. Enrichment was determined based on the double-delta CT value. Two technical replicates were used per sample. Primer list in Figure S7.

Pathway and GO functional analysis

Geneset functional analysis was conducted using Panther (http://www.pantherdb.org/), String (https://string-db.org/) and DAVID (https://david.ncifcrf.gov/). All three methods were used to obtain a more complete picture of shared regulation between datasets. KEGG pathway maps were obtained through KEGG Pathway (http://www.kegg.jp/kegg/pathway.html).

Motif analysis

Motif analysis was conducted using Homer's *findMotifsGenome* script (http://homer.ucsd.edu/homer/ngs/peakMotifs.html, [61] to compare peak regions with dm6.01 FASTA data from UCSC.

List of raw datasets used

ChIP-seq datasets: GSE62580 (Drosophila Fat body DE), GSE81100 (*Drosophila* aging head DE), GSE81221 (S2R+ FOXO RNAi RNA-seq), GSE44686 (*Drosophila Chico* heterozygotes dFOXO ChIP), GSE15567 (Encode *C. elegans Daf-16* ChIP)

Statistical analysis

bioRxiv preprint doi: https://doi.org/10.1101/456426; this version posted October 30, 2018. The copyright holder for this preprint (which was not certified by peer review) is the author/funder. All rights reserved. No reuse allowed without permission.

GraphPad Prism (GraphPad Software, La Jolla, CA, USA) was used for statistical analysis. To compare the mean value of treatment groups versus that of control, either student t-test or one-way ANOVA was performed using Dunnett's test for multiple comparison.

Acknowledgements

We thank Usha Muppirala and Andrew Severin from the Genome Informatics Facility (GIF) at Iowa State University for assistance with bioinformatics. We thank Christian Riedel for providing peak data from *C. elegans*.

Figure Legends

Figure 1. Immunofluorescent staining of dFOXO in 1 and 5-week old yellow-white flies and in 1-week old Oregon-R and *foxo*^{21} mutants. **A)** Drosophila abdominal fat body tissue stained with anti-dFOXO followed Alexa-fluor-488 and DAPI **B))** Overlap between FOX- DAPI staining in fat body tissue (***P< 0.001, ****P<0.0001) **C)** Tissue from Drosophila indirect flight muscles stained with anti-dFOXO followed Alexa-fluor-488 and DAPI. **D)** Overlap between FOX- DAPI staining in muscle tissue (*P< 0.05).

Figure 2. FOXO targeted enrichment decreases with age. A) A pictogram of the workflow used to analyze ChIP-seq reads acquired from Illumina 3000. **B)** 2-week old flies have more enriched peaks compared to 5-week old flies. Pathways enriched in younger flies contain known FOXO regulated pathways involving growth and cell cycle progression as well as pathways involving G-protein Couple Receptors. **C)** Alignment data shows enrichment of reads at FOXO targeted regions in young flies that are not present in old flies at the Aux TSS. **D)** Plot correlation

bioRxiv preprint doi: https://doi.org/10.1101/456426; this version posted October 30, 2018. The copyright holder for this preprint (which was not certified by peer review) is the author/funder. All rights reserved. No reuse allowed without permission.

Matrix shows 5 week-old flies are most similar to input samples, supporting low FOXO binding activity. **E-G)** qPCR or ChIP library samples at peak regions for insulin receptor, *Bmm* (*P<0.05), and Jim in young and old ywR flies (****P<0.0001).

Figure 3. Wild-type FOXO-bound genes unique to young flies show transcriptional changes with age. A**)** Overlap of FOXO target genes with genes altered with age in the fat body tissue. B**)** Representative biological processes enriched through gene ontology of overlapping genes with aging fat body tissue. **C)** Overlap between FOXO target genes and transcriptome data between10-60 day head tissue **D)** Representative biological processes enriched through gene ontology of overlapping genes with aging head tissue.

Figure 4. Wild-type FOXO-targets are distinct from those associated with insulin signaling. **A)** Venn diagram of wild-type and chico ChIP-seq FOXO target genes. **B)** wild-type and chico FOXO-bound genes overlapped with genes differentially expressed during aging. Differentially expressed genes were acquired from aging transcriptome data sets from the head and fat body. **C)** GO analysis for unique genesets overlapping with the aging transcriptome reflect distinct pathways that become differentially regulated with aging. **D)** Wild-type FOXO targets show little overlap with transcriptional data from insulin receptor mutants. **E)** Wild-type *C. elegans* share only a subset of overlap with *daf-2* mutants similar to wild-type and chico *Drosophila* **F)** Wild-type *Drosophila* share many pathways and processes with wild-type *C. elegans* Daf-16 targets.

bioRxiv preprint doi: https://doi.org/10.1101/456426; this version posted October 30, 2018. The copyright holder for this preprint (which was not certified by peer review) is the author/funder. All rights reserved. No reuse allowed without permission.

Figure S1. Western blotting analysis on insulin signaling in young and old wild-type and *foxo*^{21} mutants.

Figure S2. Concentration of ChIP DNA samples before library preparation.

Figure S3. Total raw reads and Bowtie alignment percentage for individual sequencing sample.

Figure S4. FOXO targets in hippo signaling pathway. Blue: Wild-type only. Pink: *Chico* mutant only. Green: Shared.

Figure S5. FOXO targets in MAPK/EGFR pathway. Blue: Wild-type only. Pink: *Chico* mutant only. Green: Shared.

Figure S6. FOXO targets in JNK signaling pathway. Blue: Wild-type only. Pink: *Chico* mutant only. Green: Shared.

Figure S7. Primers used for ChIP qPCR. Results normalized against Act5C control expression.

References:

1. Dice, J.F., *Cellular and molecular mechanisms of aging.* Physiol Rev, 1993. **73**(1): p. 149-59.
2. Cui, H., Y. Kong, and H. Zhang, *Oxidative stress, mitochondrial dysfunction, and aging.* J Signal Transduct, 2012. **2012**: p. 646354.
3.
4. Greer, E.L. and A. Brunet, *FOXO transcription factors at the interface between longevity and tumor suppression.* Oncogene, 2005. **24**(50): p. 7410-25.
5. Brunet, A., et al., *Akt promotes cell survival by phosphorylating and inhibiting a Forkhead transcription factor.* Cell, 1999. **96**(6): p. 857-68.
6. Kitamura, T., et al., *The forkhead transcription factor Foxo1 links insulin signaling to Pdx1 regulation of pancreatic beta cell growth.* J Clin Invest, 2002. **110**(12): p. 1839-47.
7. Kops, G.J., et al., *Forkhead transcription factor FOXO3a protects quiescent cells from oxidative stress.* Nature, 2002. **419**(6904): p. 316-21.
8. Martins, R., G.J. Lithgow, and W. Link, *Long live FOXO: unraveling the role of FOXO proteins in aging and longevity.* Aging Cell, 2016. **15**(2): p. 196-207.
9. Medema, R.H., et al., *AFX-like Forkhead transcription factors mediate cell-cycle regulation by Ras and PKB through p27kip1.* Nature, 2000. **404**(6779): p. 782-7.
10. Kenyon, C., et al., *A C. elegans mutant that lives twice as long as wild type.* Nature, 1993. **366**(6454): p. 461-4.
11. Holzenberger, M., et al., *IGF-1 receptor regulates lifespan and resistance to oxidative stress in mice.* Nature, 2003. **421**(6919): p. 182-7.

bioRxiv preprint doi: https://doi.org/10.1101/456426; this version posted October 30, 2018. The copyright holder for this preprint (which was not certified by peer review) is the author/funder. All rights reserved. No reuse allowed without permission.

12. Tatar, M., et al., *A mutant Drosophila insulin receptor homolog that extends life-span and impairs neuroendocrine function.* Science, 2001. **292**(5514): p. 107-10.
13. Fontana, L., S. Klein, and J.O. Holloszy, *Effects of long-term calorie restriction and endurance exercise on glucose tolerance, insulin action, and adipokine production.* Age (Dordr), 2010. **32**(1): p. 97-108.
14. Hansen, M., et al., *A role for autophagy in the extension of lifespan by dietary restriction in C. elegans.* PLoS Genet, 2008. **4**(2): p. e24.
15. Dansen, T.B. and B.M. Burgering, *Unravelling the tumor-suppressive functions of FOXO proteins.* Trends Cell Biol, 2008. **18**(9): p. 421-9.
16. Essers, M.A., et al., *FOXO transcription factor activation by oxidative stress mediated by the small GTPase Ral and JNK.* EMBO J, 2004. **23**(24): p. 4802-12.
17. Lehtinen, M.K., et al., *A conserved MST-FOXO signaling pathway mediates oxidative-stress responses and extends life span.* Cell, 2006. **125**(5): p. 987-1001.
18. Huang, H. and D.J. Tindall, *FOXO factors: a matter of life and death.* Future Oncol, 2006. **2**(1): p. 83-9.
19. Alic, N., et al., *Genome-wide dFOXO targets and topology of the transcriptomic response to stress and insulin signalling.* Mol Syst Biol, 2011. **7**: p. 502.
20. Junger, M.A., et al., *The Drosophila forkhead transcription factor FOXO mediates the reduction in cell number associated with reduced insulin signaling.* J Biol, 2003. **2**(3): p. 20.
21. Riedel, C.G., et al., *DAF-16 employs the chromatin remodeller SWI/SNF to promote stress resistance and longevity.* Nat Cell Biol, 2013. **15**(5): p. 491-501.
22. Puig, O., et al., *Control of cell number by Drosophila FOXO: downstream and feedback regulation of the insulin receptor pathway.* Genes Dev, 2003. **17**(16): p. 2006-20.
23. Hossain, M.S., et al., *20-Hydroxyecdysone-induced transcriptional activity of FoxO upregulates brummer and acid lipase-1 and promotes lipolysis in Bombyx fat body.* Insect Biochem Mol Biol, 2013. **43**(9): p. 829-38.
24. Kang, P., et al., *Drosophila Kruppel homolog 1 represses lipolysis through interaction with dFOXO.* Sci Rep, 2017. **7**(1): p. 16369.
25. Bai, H., et al., *Activin signaling targeted by insulin/dFOXO regulates aging and muscle proteostasis in Drosophila.* PLoS Genet, 2013. **9**(11): p. e1003941.
26. Murphy, L.J., *Insulin-like growth factor-I: a treatment for type 2 diabetes revisited.* Endocrinology, 2006. **147**(6): p. 2616-8.
27. Webb, A.E., A. Kundaje, and A. Brunet, *Characterization of the direct targets of FOXO transcription factors throughout evolution.* Aging Cell, 2016. **15**(4): p. 673-85.
28. Furuyama, T., et al., *Identification of the differential distribution patterns of mRNAs and consensus binding sequences for mouse DAF-16 homologues.* Biochemical Journal, 2000. **349**: p. 629-634.
29. Webb, A.E., et al., *FOXO3 shares common targets with ASCL1 genome-wide and inhibits ASCL1-dependent neurogenesis.* Cell Rep, 2013. **4**(3): p. 477-91.
30. Eijkelenboom, A., et al., *FOXO3 selectively amplifies enhancer activity to establish target gene regulation.* Cell Rep, 2013. **5**(6): p. 1664-78.
31. Hwangbo, D.S., et al., *Drosophila dFOXO controls lifespan and regulates insulin signalling in brain and fat body.* Nature, 2004. **429**(6991): p. 562-6.
32. Willcox, B.J., et al., *FOXO3A genotype is strongly associated with human longevity.* Proc Natl Acad Sci U S A, 2008. **105**(37): p. 13987-92.
33. Schuster, E., et al., *DamID in C. elegans reveals longevity-associated targets of DAF-16/FoxO.* Mol Syst Biol, 2010. **6**: p. 399.

bioRxiv preprint doi: https://doi.org/10.1101/456426; this version posted October 30, 2018. The copyright holder for this preprint (which was not certified by peer review) is the author/funder. All rights reserved. No reuse allowed without permission.

34. Teleman, A.A., et al., *Nutritional control of protein biosynthetic capacity by insulin via Myc in Drosophila.* Cell Metab, 2008. **7**(1): p. 21-32.
35. Brenkman, A.B., et al., *Mdm2 induces mono-ubiquitination of FOXO4.* PLoS One, 2008. **3**(7): p. e2819.
36. Brunet, A., et al., *Stress-dependent regulation of FOXO transcription factors by the SIRT1 deacetylase.* Science, 2004. **303**(5666): p. 2011-5.
37. Sekine, K., et al., *Foxo1 links insulin signaling to C/EBPalpha and regulates gluconeogenesis during liver development.* EMBO J, 2007. **26**(15): p. 3607-15.
38. Daitoku, H., J. Sakamaki, and A. Fukamizu, *Regulation of FoxO transcription factors by acetylation and protein-protein interactions.* Biochim Biophys Acta, 2011. **1813**(11): p. 1954-60.
39. van der Vos, K.E. and P.J. Coffer, *FOXO-binding partners: it takes two to tango.* Oncogene, 2008. **27**(16): p. 2289-99.
40. Zhong, M., et al., *Genome-wide identification of binding sites defines distinct functions for Caenorhabditis elegans PHA-4/FOXA in development and environmental response.* PLoS Genet, 2010. **6**(2): p. e1000848.
41. Olmos, Y., et al., *Mutual dependence of Foxo3a and PGC-1alpha in the induction of oxidative stress genes.* J Biol Chem, 2009. **284**(21): p. 14476-84.
42. Polvani, S., M. Tarocchi, and A. Galli, *PPARgamma and Oxidative Stress: Con(beta) Catenating NRF2 and FOXO.* PPAR Res, 2012. **2012**: p. 641087.
43. Armoni, M., et al., *FOXO1 represses peroxisome proliferator-activated receptor-gamma1 and -gamma2 gene promoters in primary adipocytes. A novel paradigm to increase insulin sensitivity.* J Biol Chem, 2006. **281**(29): p. 19881-91.
44. Klotz, L.O., et al., *Redox regulation of FoxO transcription factors.* Redox Biol, 2015. **6**: p. 51-72.
45. Singh, B.K., et al., *Hepatic FOXO1 Target Genes Are Co-regulated by Thyroid Hormone via RICTOR Protein Deacetylation and MTORC2-AKT Protein Inhibition.* J Biol Chem, 2016. **291**(1): p. 198-214.
46. van der Horst, A. and B.M. Burgering, *Stressing the role of FoxO proteins in lifespan and disease.* Nat Rev Mol Cell Biol, 2007. **8**(6): p. 440-50.
47. Accili, D. and K.C. Arden, *FoxOs at the crossroads of cellular metabolism, differentiation, and transformation.* Cell, 2004. **117**(4): p. 421-6.
48. Mao, B., et al., *Hippo signaling in stress response and homeostasis maintenance.* Acta Biochim Biophys Sin (Shanghai), 2015. **47**(1): p. 2-9.
49. Udan, R.S., et al., *Hippo promotes proliferation arrest and apoptosis in the Salvador/Warts pathway.* Nat Cell Biol, 2003. **5**(10): p. 914-20.
50. Zhou, Y., et al., *Growth control of multiple myeloma cells through inhibition of glycogen synthase kinase-3.* Leuk Lymphoma, 2008. **49**(10): p. 1945-53.
51. Heallen, T., et al., *Hippo signaling impedes adult heart regeneration.* Development, 2013. **140**(23): p. 4683-90.
52. Jiang, H., et al., *EGFR/Ras/MAPK signaling mediates adult midgut epithelial homeostasis and regeneration in Drosophila.* Cell Stem Cell, 2011. **8**(1): p. 84-95.
53. Lee, Y.M. and Y.H. Sun, *Maintenance of glia in the optic lamina is mediated by EGFR signaling by photoreceptors in adult Drosophila.* PLoS Genet, 2015. **11**(4): p. e1005187.
54. Hazan, R.B. and L. Norton, *The epidermal growth factor receptor modulates the interaction of E-cadherin with the actin cytoskeleton.* J Biol Chem, 1998. **273**(15): p. 9078-84.
55. Tan, X., et al., *Stress-Induced EGFR Trafficking: Mechanisms, Functions, and Therapeutic Implications.* Trends Cell Biol, 2016. **26**(5): p. 352-366.
56. Larson, J.L. and G.C. Yuan, *Chromatin states accurately classify cell differentiation stages.* PLoS One, 2012. **7**(2): p. e31414.

bioRxiv preprint doi: https://doi.org/10.1101/456426; this version posted October 30, 2018. The copyright holder for this preprint (which was not certified by peer review) is the author/funder. All rights reserved. No reuse allowed without permission.

538 57. Wood, J.G., et al., *Chromatin remodeling in the aging genome of Drosophila.* Aging Cell, 2010.
539 **9**(6): p. 971-8.
540 58. Zhang, W., et al., *Aging stem cells. A Werner syndrome stem cell model unveils heterochromatin*
541 *alterations as a driver of human aging.* Science, 2015. **348**(6239): p. 1160-3.
542 59. Schindelin, J., et al., *Fiji: an open-source platform for biological-image analysis.* Nat Methods,
543 2012. **9**(7): p. 676-82.
544 60. Feng, J., et al., *Identifying ChIP-seq enrichment using MACS.* Nat Protoc, 2012. **7**(9): p. 1728-40.
545 61. Heinz, S., et al., *Simple combinations of lineage-determining transcription factors prime cis-*
546 *regulatory elements required for macrophage and B cell identities.* Mol Cell, 2010. **38**(4): p. 576-
547 89.

548

bioRxiv preprint doi: https://doi.org/10.1101/456426; this version posted October 30, 2018. The copyright holder for this preprint (which was not certified by peer review) is the author/funder. All rights reserved. No reuse allowed without permission.

Figure 1

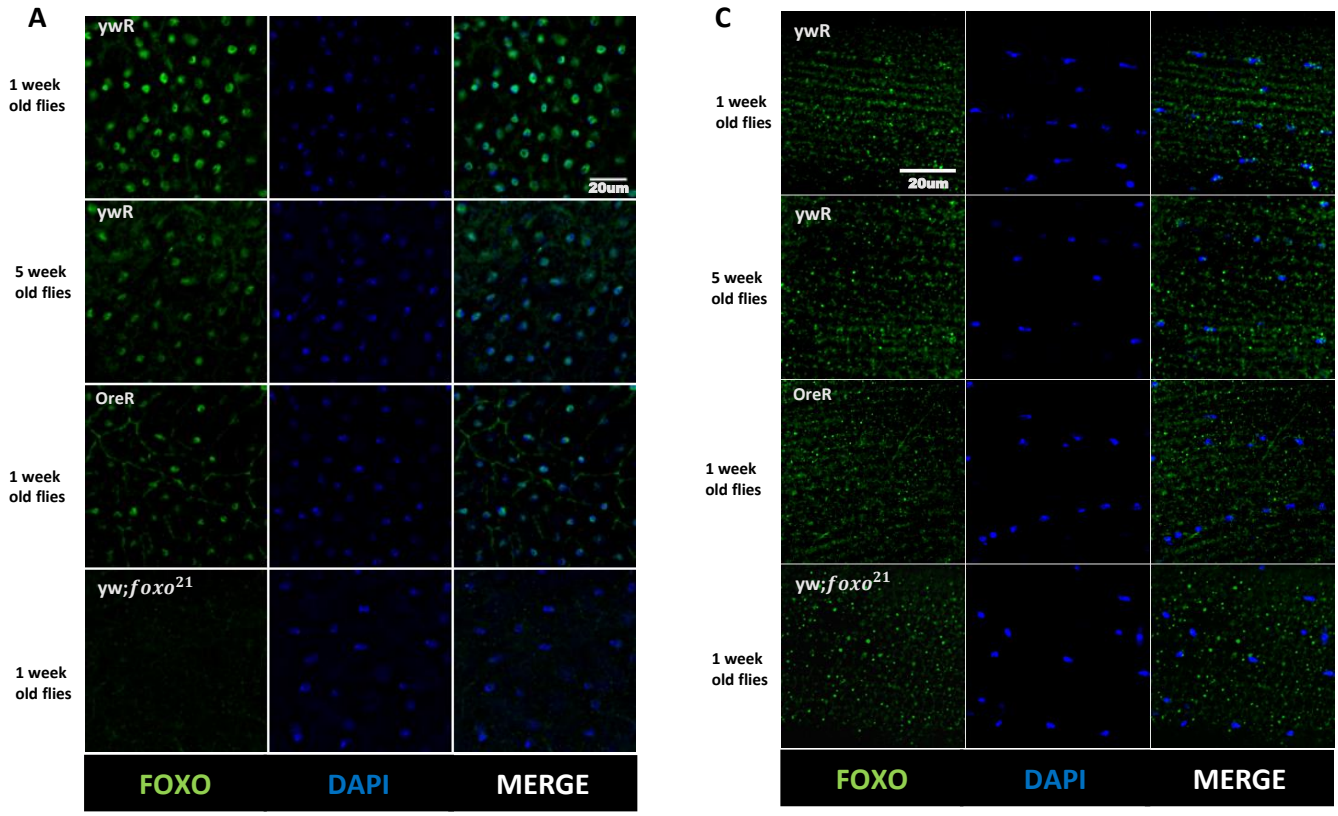

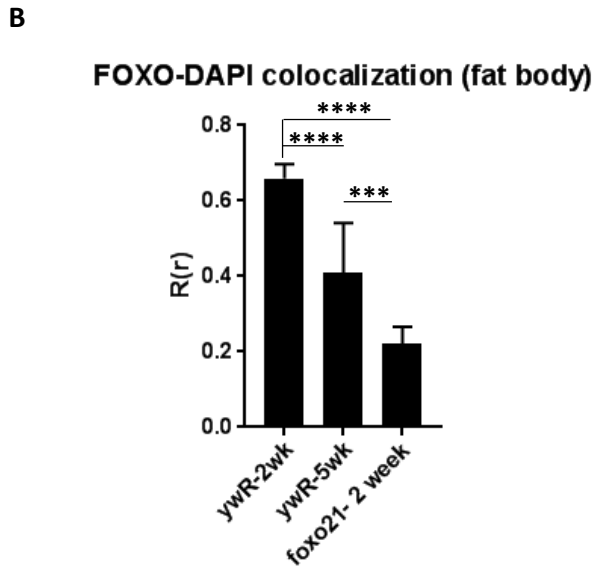

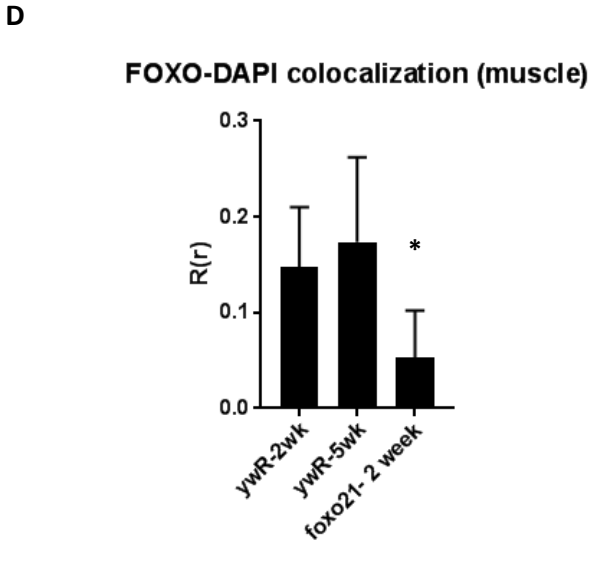

bioRxiv preprint doi: https://doi.org/10.1101/456426; this version posted October 30, 2018. The copyright holder for this preprint (which was not certified by peer review) is the author/funder. All rights reserved. No reuse allowed without permission.

Figure 2

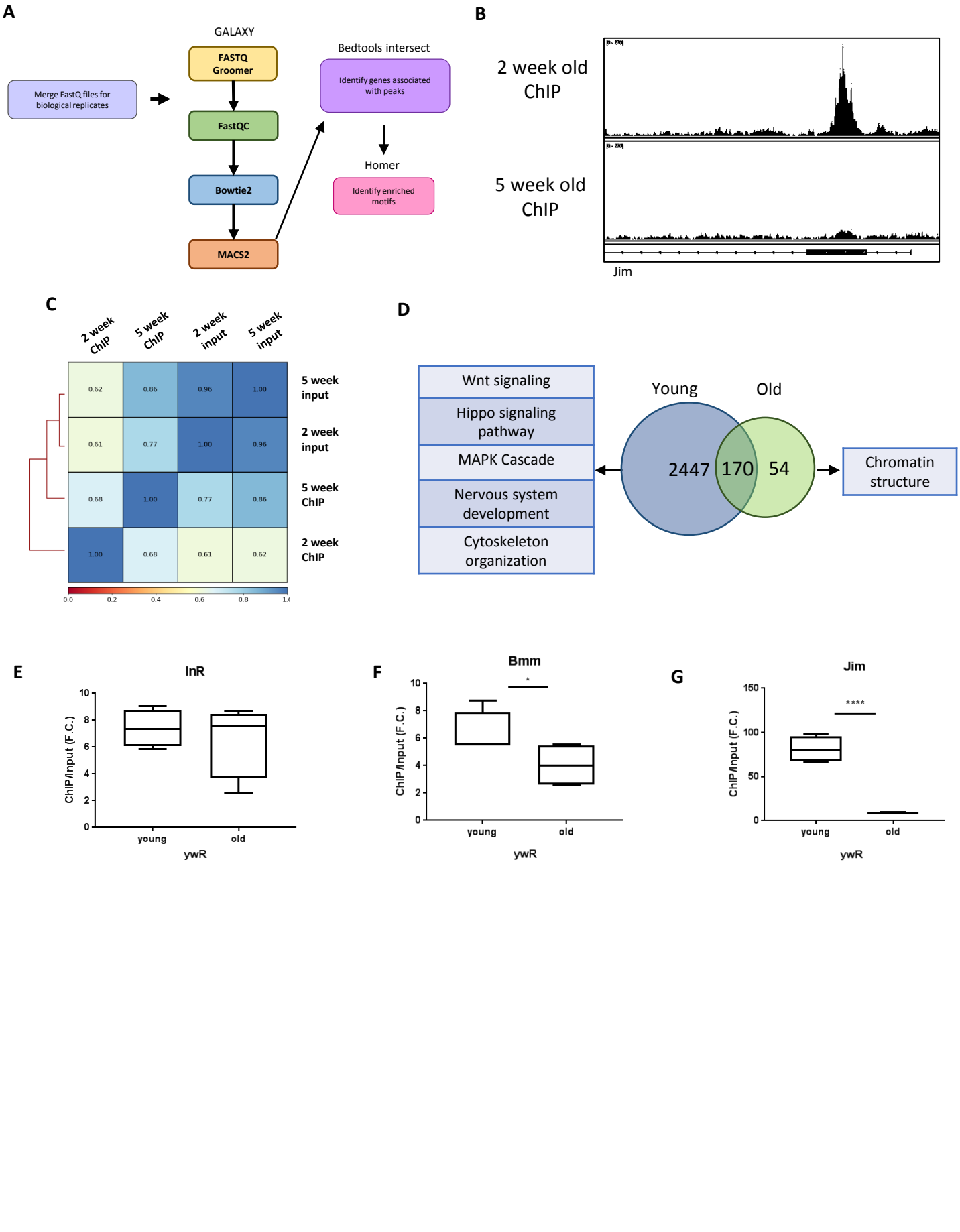

bioRxiv preprint doi: https://doi.org/10.1101/456426; this version posted October 30, 2018. The copyright holder for this preprint (which was not certified by peer review) is the author/funder. All rights reserved. No reuse allowed without permission.

Figure 3

A

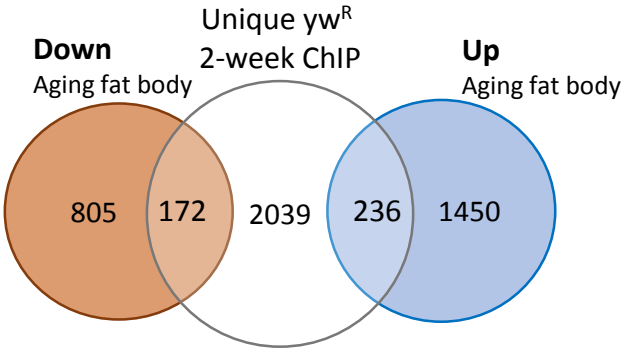

B

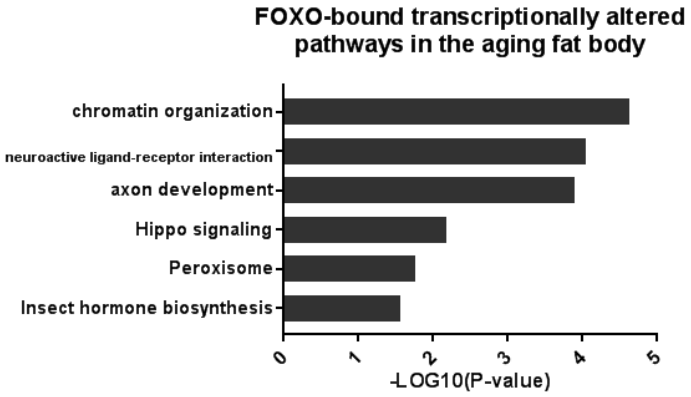

C

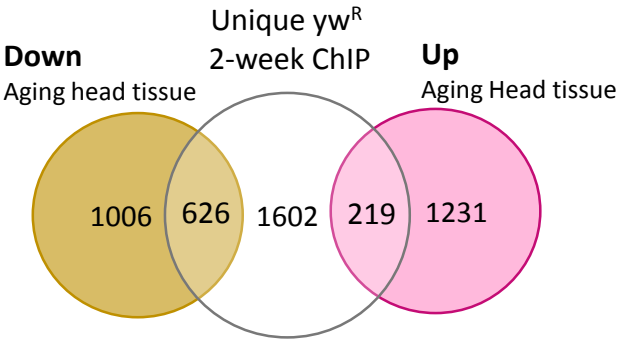

D

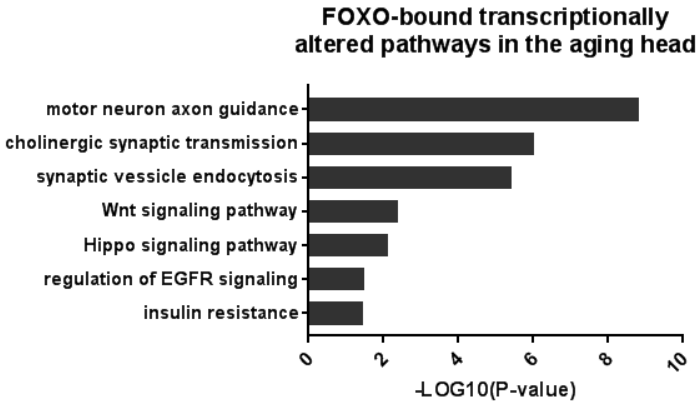

bioRxiv preprint doi: https://doi.org/10.1101/456426; this version posted October 30, 2018. The copyright holder for this preprint (which was not certified by peer review) is the author/funder. All rights reserved. No reuse allowed without permission.

Figure 4

A

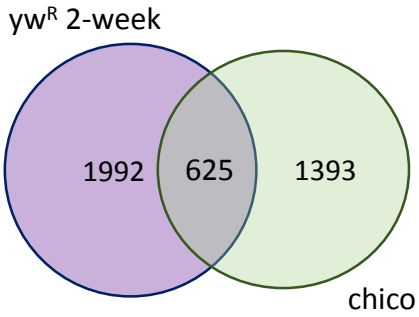

B

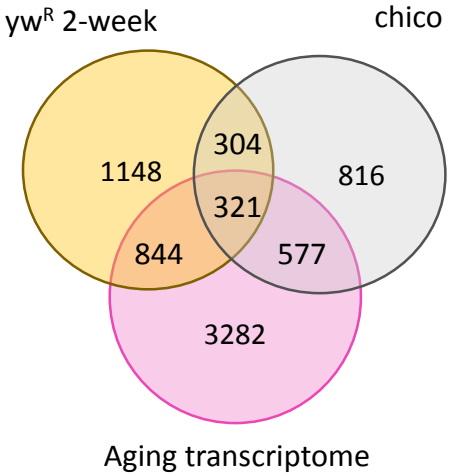

C

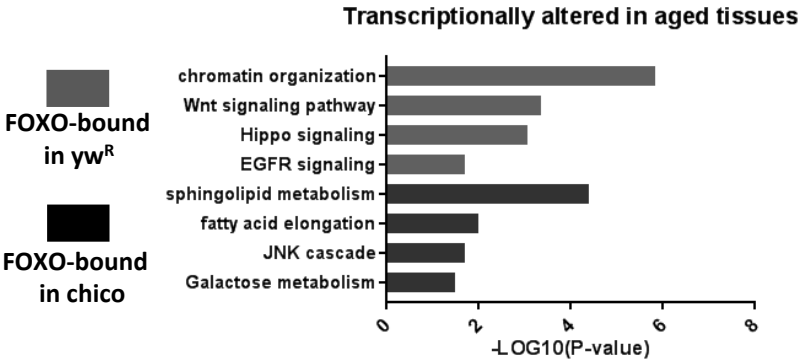

D

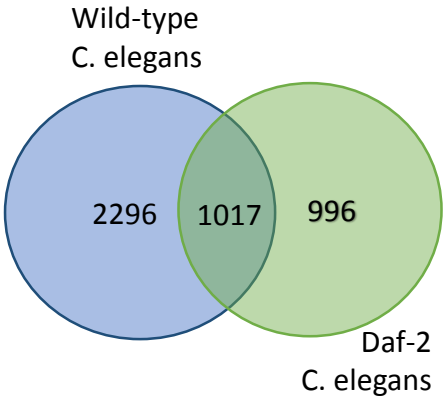

E

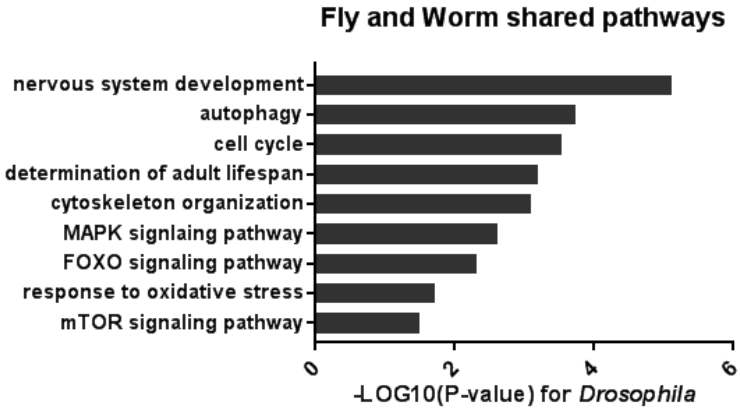

bioRxiv preprint doi: https://doi.org/10.1101/456426; this version posted October 30, 2018. The copyright holder for this preprint (which was not certified by peer review) is the author/funder. All rights reserved. No reuse allowed without permission.

Table 1

motif	P-value	# targets with motif	predicted to be bound by
Enriched known binding motifs compared to whole genome			
	1.00E-70	842	Trl(Zf)/S2-GAGAfactor
motif	**P-value**	**% targets with motif**	**predicted to be bound by**
Enriched *de novo* binding motifs compared to whole genome			
	1.00E-164	47.58%	RAP1/MA0359.1/Jaspar(0.703
	1.00E-130	44.94%	hb/dmmpmm(Noyes)/fly(0.726)
	1.00E-82	35.48%	Adf1/dmmpmm(Bergman)/fly(0.664)
	1.00E-56	27.59%	Aef1/dmmpmm(Pollard)/fly(0.851)
motif	**P-value**	**# targets with motif**	**predicted to be bound by**
Enriched known binding motifs all organisms			
	1.00E-04	1012	Foxo1(Forkhead)/RAW-Foxo1-ChIP-Seq(Fan_et_al.)/Homer

bioRxiv preprint doi: https://doi.org/10.1101/456426; this version posted October 30, 2018. The copyright holder for this preprint (which was not certified by peer review) is the author/funder. All rights reserved. No reuse allowed without permission.

Figure S1

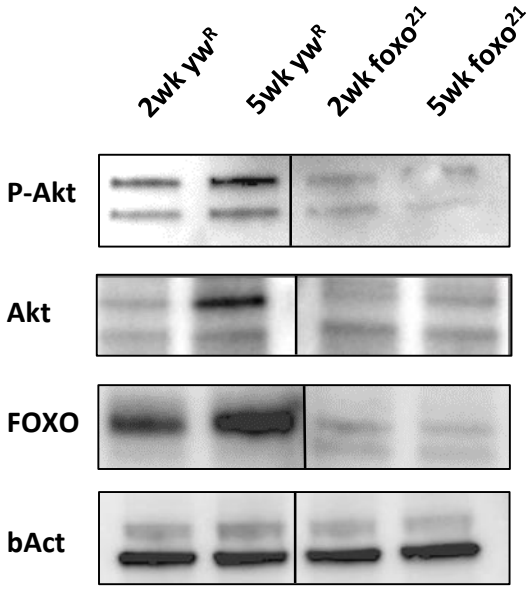

bioRxiv preprint doi: https://doi.org/10.1101/456426; this version posted October 30, 2018. The copyright holder for this preprint (which was not certified by peer review) is the author/funder. All rights reserved. No reuse allowed without permission.

Figure S2

Sample	Concentration
ywR 2-week old ChIP-1	7.49 ng/ul
ywR 2-week old input-1	35.9 ng/ul
ywR 2-week old ChIP-2	6.41 ng/ul
ywR 2-week old input-2	26.6 ng/ul
ywR 5-week old ChIP-1	20.2 ng/ul
ywR 5-week old input-1	32.1 ng/ul
ywR 5-week old ChIP-2	8.79 ng/ul
ywR 5-week old input-2	26.7 ng/ul

bioRxiv preprint doi: https://doi.org/10.1101/456426; this version posted October 30, 2018. The copyright holder for this preprint (which was not certified by peer review) is the author/funder. All rights reserved. No reuse allowed without permission.

Figure S3

Sample	Raw reads	% Alignment
ywR 2-week old ChIP-1	25554421	85.74%
ywR 2-week old input-1	40459444	96.09%
ywR 2-week old ChIP-2	15933943	73.70%
ywR 2-week old input-2	34196540	96.26%
ywR 5-week old ChIP-1	15880701	92.00%
ywR 5-week old input-1	73535040	95.06%
ywR 5-week old ChIP-2	14515822	91.76%
ywR 5-week old input-2	40815124	95.98%

bioRxiv preprint doi: https://doi.org/10.1101/456426; this version posted October 30, 2018. The copyright holder for this preprint (which was not certified by peer review) is the author/funder. All rights reserved. No reuse allowed without permission.

Figure S4

Hippo Signaling Pathway

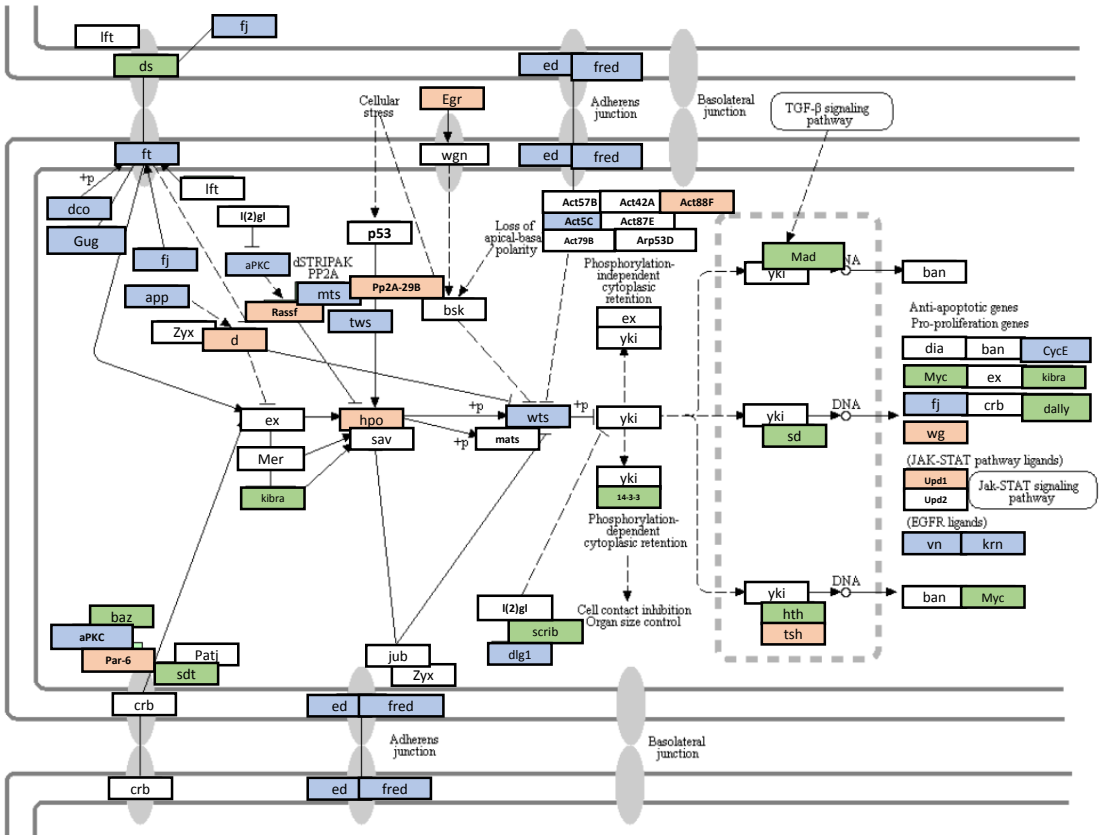

bioRxiv preprint doi: https://doi.org/10.1101/456426; this version posted October 30, 2018. The copyright holder for this preprint (which was not certified by peer review) is the author/funder. All rights reserved. No reuse allowed without permission.

Figure S5

EGFR Pathway

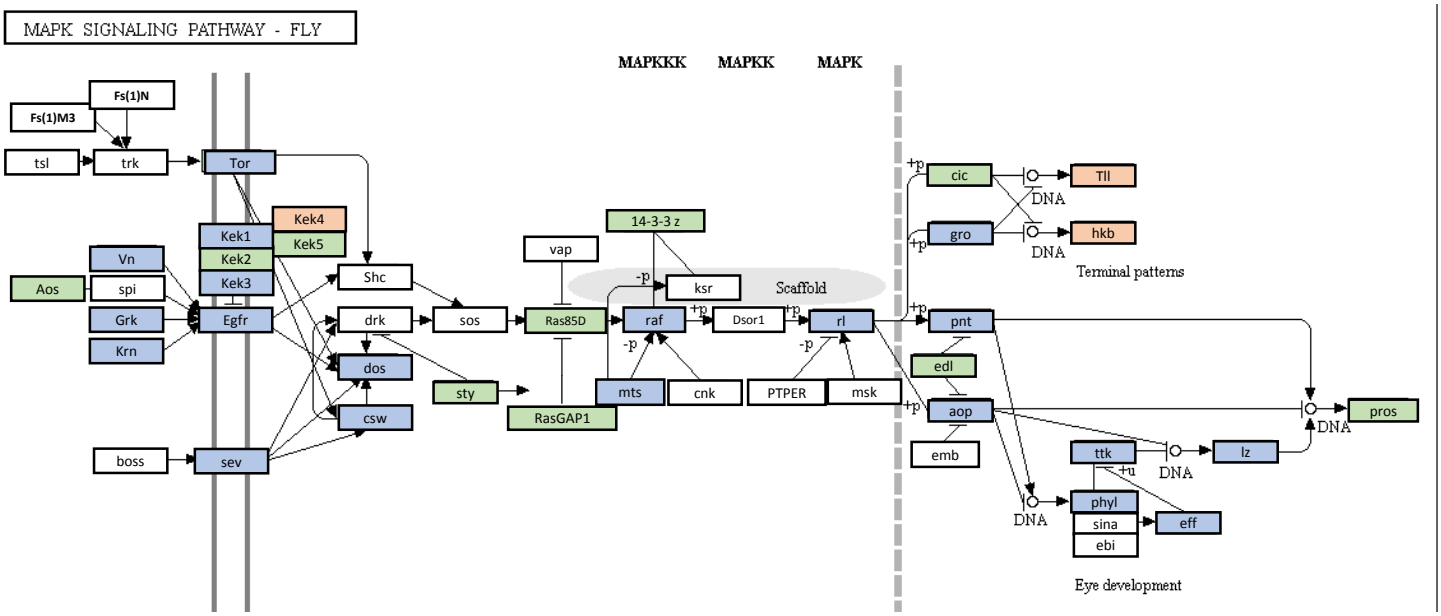

bioRxiv preprint doi: https://doi.org/10.1101/456426; this version posted October 30, 2018. The copyright holder for this preprint (which was not certified by peer review) is the author/funder. All rights reserved. No reuse allowed without permission.

Figure S6

JNK Pathway

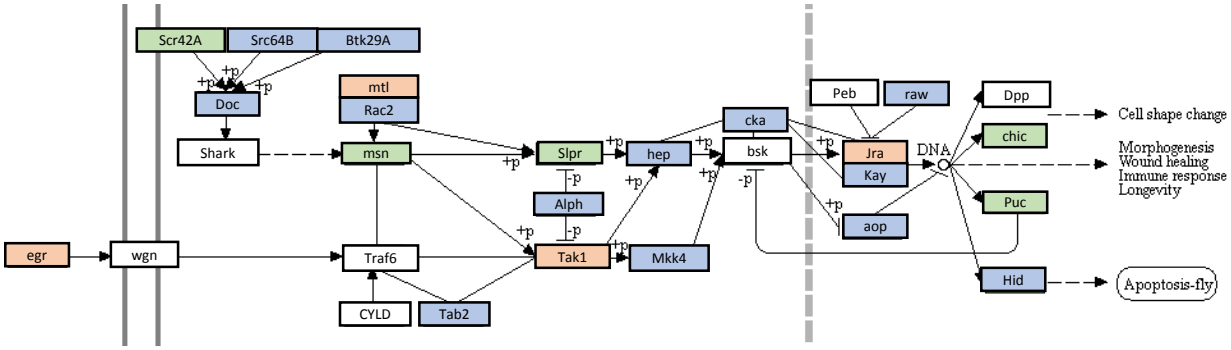

bioRxiv preprint doi: https://doi.org/10.1101/456426; this version posted October 30, 2018. The copyright holder for this preprint (which was not certified by peer review) is the author/funder. All rights reserved. No reuse allowed without permission.

Figure S7

Gene	Direction	Sequence 5'->3'
Act5C	Forward	TCGCGATTTGACCGACTACCTGAT
	Reverse	TGATGTCACGGACGATTTCACGCT
InR-prom974	Forward	ATAGAACGACGCACTTTCCC
	Reverse	CGCGCGCTCTCCTATTATTTA
Bmm-prom1	Forward	CACCGCGCCGCAATGAATGTATAA
	Reverse	TTCAATCACTGTTTGTCGGTCGGC
Jim	Forward	GAGGCGGGTTTAAGGCTATT
	Reverse	CAGGCAAACAAATCAAAGCAAAC